Adaptive Control of Hammerstein Systems with Unknown Input Nonlinearity and Partially Modeled Linear Dynamics

Mohammad Al Janaideh and Dennis S. Bernstein

Adaptive Control of Hammerstein Systems with Unknown Input Nonlinearity and Partially Modeled Linear Dynamics

Mohammad Al Janaideh* and Dennis S. Bernstein

Abstract: We numerically investigate that an adaptive control law achieves internal model principle control in the presence of plant input nonlinearities. We focus on retrospective cost adaptive control (RCAC) applied to Hammerstein systems with unknown input nonlinearity and limited modeling of the linear dynamics. The goal is to determine whether the control law achieves the correct gain and phase shift for internal stability along with asymptotic command following and disturbance rejection.

Keywords: Adaptive control, nonlinear systems.

1. INTRODUCTION

The internal model principle (IMP) states that a stabilizing control law that achieves asymptotically perfect command following or disturbance rejection must "possess" a model of the exogenous signal [1–3]. IMP is the basis for PID control, whose integrator can be viewed as a model of a step command or step disturbance [4]. It is worth noting that, in a classical servo loop where the objective is command following, the requirement for an internal model in the loop transfer function can be satisfied by the plant itself, but this is not the case for disturbance rejection. For example, asymptotic command following for a step command with a plant that has a pole at zero can be achieved by any stabilizing controller, but rejection of a step disturbance requires that the controller provide integral action.

In the present paper we revisit IMP control within the context of adaptive control of Hammerstein systems. In addition to uncertainty in the linear dynamics and input nonlinearity, the nonlinearity induces additional, undesirable harmonic content in the plant input. The adaptive controller must account for these harmonics in following the command.

In [5], retrospective cost adaptive control (RCAC) with auxiliary nonlinearities is presented to address a command-following problem for uncertain Hammerstein systems with possibly non-monotonic input nonlinearities. Papers [6] and [7] apply retrospective cost adaptive control (RCAC) to a command-following problem for uncertain systems with hysteresis nonlinearities. These papers numerically investigate that an adaptive control law achieves IMP control of Hammerstein plants with Duhem and Prandtl–Ishlinskii hysteresis nonlinearities. The approach uses the phase shift to determine whether the adaptive controller inverts the plant.

The goal of the present paper is to numerically investigate the ability of RCAC to achieve IMP control in the presence of plant input memoryless nonlinearities. Although we focus on RCAC, the methodology that we use to analyze the controller action can be applied to any control law that achieves internal stability along with either command following or disturbance rejection. Furthermore, although we focus on discrete-time (possibly sampled-data) plants, the ideas are applicable to continuous-time systems.

Of special interest is the operation of the control law in terms of phase compensation. Since asymptotically perfect command following for linear systems requires that the plant output match the phase and amplitude of the sinusoidal command, the plant input must also be a sinusoid and its amplitude and phase must be consistent with the magnitude and phase shift of the plant at the command frequency. However, the phase of the control input cannot be determined by examining the phase shift of the controller due to the fact that, at the command frequency, the controller has a phase discontinuity. In continuous time, this discontinuity is 180 degrees at non-DC command frequencies due to poles on the imaginary axis, whereas, in discrete time, the discontinuity is 360 degrees due to poles on the unit circle.

Mohammad Al Janaideh is with the Department of Mechanical and Industrial Engineering, The Mechatronics and Microsystems Design Laboratory, University of Toronto, Canada, and the Department of Mechatronics Engineering, Faculty of Engineering and Technology, The University of Jordan, Amman 11942, Jordan (e-mail: aljanaideh@gmail.com). Dennis S. Bernstein is with the Department of Aerospace Engineering, The University of Michigan, Ann Arbor, MI 48109, USA (e-mail: dsbaero@umich.edu).
* Corresponding author.

Since, due to the discontinuity, the controller phase cannot be used as a diagnostic for IMP control, we consider instead the transfer function G_{ur} from the command r to the control input u. When cascaded with the plant G, the resulting transfer function must be unity, that is, a magnitude of 1 with zero phase shift, at the command frequency. This means that the transfer functions G_{ur} and G in cascade must be mutual inverses at the command frequency. We use this diagnostic to analyze adaptive control laws, but we also consider the contribution of the harmonics to the command-following error. For Hammerstein systems, we use describing functions to estimate the phase shift and magnitude of the input nonlinearity at the command frequency.

2. PROBLEM FORMULATION

In this section we begin with fixed gain control for a classical servo loop with harmonic commands. For a SISO LTI plant, we choose an IMP control under the assumption that the command frequency is known. We then show that the control law places a zero on the unit circle in the transfer function from the reference r to the command-following error e. The presence of this zero illustrates the operation of the IMP control. Equivalently, the final value theorem shows that the controller applies infinite gain at the command frequency, thus driving the command-following error to zero. Consider the linear system

$$x(k+1) = Ax(k) + Bu(k), \tag{1}$$
$$e(k) = y(k) - r(k), \tag{2}$$
$$y(k) = Cx(k), \tag{3}$$

where $x(k) \in \mathbb{R}^n$ is the state, $y(k) \in \mathbb{R}$ is the measured output available to the controller, $e(k) \in \mathbb{R}$ is the command-following error, $u(k) \in \mathbb{R}$ is the control, and $r(k) \in \mathbb{R}$ is the command input. The goal is to determine u that makes e close to zero.

The closed-loop system presented in Fig. 1 can be represented by the cascaded system in Fig. 2, where

$$G_{ur} = \frac{G_c}{1 + G_c G}. \tag{4}$$

Suppose that the system shown in Fig. 2 is driven by the command signal $r(k) = \text{Re}\{A_r e^{j\Omega k}\}$, where A_r is a complex number. Then the harmonic control input to the system G can be expressed as

$$u(k) = |G_{ur}(e^{j\Omega})|\text{Re}\{A_r e^{j(\Omega k + \angle G_{ur}(e^{j\Omega}))}\}, \tag{5}$$

where $|G_{ur}(e^{j\Omega})|$ and $\angle G_{ur}(e^{j\Omega})$ are the gain and phase of G_{ur}, respectively. Then

$$y(k) = |G_{ur}(e^{j\Omega})||G(e^{j\Omega})|\text{Re}\{A_r e^{j[\Omega k + \angle G_{ur}(e^{j\Omega}) + \angle G(e^{j\Omega})]}\}. \tag{6}$$
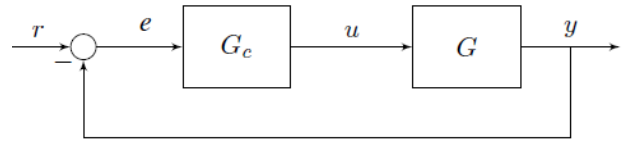
Fig. 1. Command-following problem for the linear plant G.
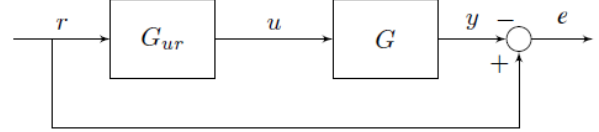
Fig. 2. Representation of the command-following problem as a cascaded system, where $G_{ur} = \frac{G_c}{1+G_c G}$.

To regulate the command-following error e to 0 at the frequency Ω, it follows that y is harmonic and $e = 0$ if and only if

$$y(k) = G(e^{j\Omega})G_{ur}(e^{j\Omega})r(k), \tag{7}$$

which is equivalent to

$$G_{ur}(e^{j\Omega})G(e^{j\Omega}) = 1. \tag{8}$$

The gain and phase of G_{ur} therefore must satisfy

$$|G_{ur}(e^{j\Omega})| = \frac{1}{|G(e^{j\Omega})|}, \tag{9}$$

$$\angle G_{ur}(e^{j\Omega}) = -\angle G(e^{j\Omega}). \tag{10}$$

Example 1: Let $r(k) = \sin(\frac{\pi}{5}k)$, the asymptotically stable linear plant $G(z) = \frac{z-0.5}{(z-0.8)(z-0.6)}$, and the controller $G_c(z) = 0.3693\frac{z}{z^2-1.902z+1}$. Note that G_c possesses an IMP model of the command signal. Fig. 3 shows that the error decreases to zero and that G_{ur} inverts the plant G at the command frequency $\Omega = \frac{\pi}{5}$ rad/sample.

3. ADAPTIVE CONTROL OF HAMMERSTEIN PLANTS

3.1. Hammerstein command-following problem

In this section we consider the Hammerstein plant

$$x(k+1) = Ax(k) + B\mathcal{N}(u(k)), \tag{11}$$
$$v(k) = \mathcal{N}(u(k)), \tag{12}$$
$$e(k) = y(k) - r(k), \tag{13}$$
$$y(k) = Cx(k), \tag{14}$$

where $\mathcal{N} : \mathbb{R} \to \mathbb{R}$, see Fig. 4. The goal is to develop an adaptive output feedback controller that minimizes the command-following error e with minimal modeling information about the plant G, and input nonlinearity $\mathcal{N}$. We assume that measurements of $y(k)$ are available for feedback; however, measurements of $v(k) = \mathcal{N}(u(k))$ are not available.

(a)   (b)

(c)
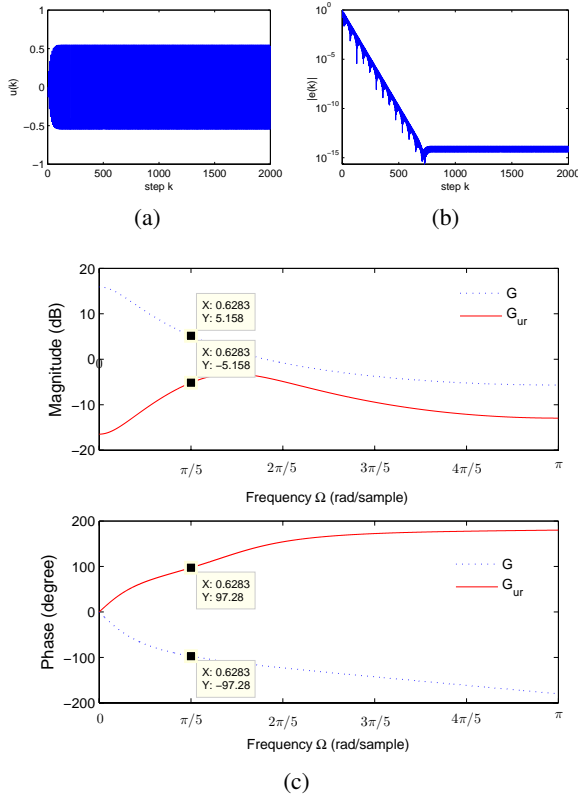
Fig. 3. Example 1: (a) shows the control signal $u(k)$, (b) the command-following error $e(k)$, (c) the bode plots of $G(z) = \frac{z-0.5}{(z-0.8)(z-0.6)}$ and $G_{ur} = \frac{G_c}{1+GG_c}$, where $G_c(z) = 0.3693 \frac{z}{z^2-1.902z+1}$. The figure shows that the magnitude and phase of G_{ur} compensate for the magnitude and phase of G at $\Omega = \pi/5$ rad/sample.
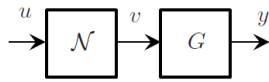
Fig. 4. The Hammerstein system $\mathcal{H}$, where $\mathcal{N}$ is the non-linearity and G is the linear plant.

3.2. The adaptive RCAC controller

The Adaptive RCAC Controller has been used in different applications [8, 9]. Various techniques have been used to control Hammerstein systems with uncertain input non-linearities and linear dynamics [10]- [12]. In this paper we focus on RCAC adaptive control, which has been used for MIMO, nonminimum phase (NMP), unstable, and Hammerstein systems, see [13]- [17]. This approach relies on knowledge of Markov parameters. In this section we present the adaptive RCAC controller used to formulate G_{ur}. Consider the controller of order n_c

$$u(k) = \sum_{i=1}^{n_c} M_i(k)u(k-i) + \sum_{i=1}^{n_c} N_i(k)e(k-i), \quad (15)$$
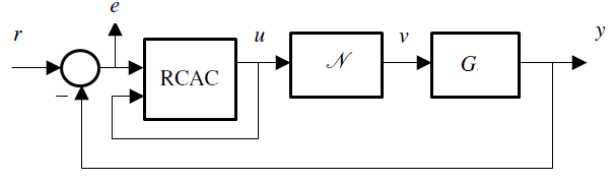
Fig. 5. Hammerstein command-following problem with the RCAC adaptive controller. The Hammerstein system consists of the input nonlinearity $\mathcal{N}$ cascaded with the linear plant G, where u is the control signal. The measurements of $y(k)$ are available for feedback; however, the measurements of $v(k) = \mathcal{N}(u(k))$ are not available.

where, for all $i = 1, \ldots, n_c$, $M_i(k) \in \mathbb{R}$, and $N_i(k) \in \mathbb{R}$. The control (15) can be expressed as

$$u(k) = \theta(k)\phi(k-1), \quad (16)$$

where

$$\theta(k) = \begin{bmatrix} M_1(k) \cdots M_{n_c}(k) & N_1(k) \cdots N_{n_c}(k) \end{bmatrix}$$

is the controller gain matrix $\theta(k) \in \mathbb{R}^{1 \times 2n_c}$, and the regressor vector $\phi(k) \in \mathbb{R}^{2n_c}$ is given by

$$\phi(k-1) = [u(k-1) \cdots u(k-n_c) \quad e(k-1) \cdots e(k-n_c)]^{\mathrm{T}}. \quad (17)$$

The transfer function matrix $G_{c,k}(\mathbf{q})$ from e to u at time step k can be represented by

$$\frac{N_1(k)\mathbf{q}^{n_c-1} + N_2(k)\mathbf{q}^{n_c-2} + \cdots + N_{n_c}(k)}{\mathbf{q}^{n_c} - \left(M_1(k)\mathbf{q}^{n_c-1} + \cdots + M_{n_c-1}(k)\mathbf{q} + M_{n_c}(k)\right)}.$$

3.3. Retrospective cost adaptive control

For $i \geq 1$, define the Markov parameter

$$H_i \triangleq CA^{i-1}B.$$

For example,

$$H_1 = CB, H_2 = CAB.$$

Let ℓ be a positive integer. Then, for all $k \geq \ell$,

$$x(k) = A^\ell x(k-\ell) + \sum_{i=1}^{\ell} A^{i-1}B\mathcal{N}(u(k-i)), \quad (18)$$

and thus

$$e(k) = CA^\ell x(k-\ell) - r(k) + \bar{H}\bar{U}(k-1), \quad (19)$$

where

$$\bar{H} \triangleq \begin{bmatrix} H_1 & \cdots & H_\ell \end{bmatrix} \in \mathbb{R}^{1 \times \ell},$$

$$\bar{U}(k-1) \triangleq \begin{bmatrix} \mathcal{N}(u(k-1)) \\ \vdots \\ \mathcal{N}(u(k-\ell)) \end{bmatrix}.$$

Next, we rearrange the columns of $\bar{H}$ and the components of $\bar{U}(k-1)$ and partition the resulting matrix and vector so that

$$\bar{H}\bar{U}(k-1) = \mathcal{H}'U'(k-1) + \mathcal{H}U(k-1), \qquad (20)$$

where $\mathcal{H}' \in \mathbb{R}^{1\times(\ell-l_U)}$, $\mathcal{H} \in \mathbb{R}^{1\times l_U}$, $U'(k-1) \in \mathbb{R}^{\ell-l_U}$, and $U(k-1) \in \mathbb{R}^{l_U}$. Then, we can rewrite (19) as

$$e(k) = \mathcal{S}(k) + \mathcal{H}U(k-1), \qquad (21)$$

where

$$\mathcal{S}(k) \triangleq CA^{\ell}x(k-\ell) - r(k) + \mathcal{H}'U'(k-1). \qquad (22)$$

Next, we define the *retrospective performance*

$$\hat{e}(k) = e(k) - \mathcal{H}U(k-1) + \mathcal{H}\hat{U}(k-1). \qquad (23)$$

Finally, we define the *retrospective cost function*

$$J(\hat{U}(k-1),k) \triangleq \hat{e}^2(k). \qquad (24)$$

The goal is to determine refined controls $\hat{U}(k-1)$ that would have provided better performance than the controls $U(k)$ that were applied to the system. The refined control values $\hat{U}(k-1)$ are subsequently used to update the controller. Next, to ensure that (24) has a global minimizer, we consider the regularized cost

$$\bar{J}(\hat{U}(k-1),k) \triangleq \hat{e}^2(k) + \eta(k)\hat{U}^{\mathrm{T}}(k-1)\hat{U}(k-1), \qquad (25)$$

where $\eta(k) \geq 0$. Substituting (23) into (25) yields

$$\bar{J}(\hat{U}(k-1),k) = \hat{U}(k-1)^{\mathrm{T}}\mathcal{A}(k)\hat{U}(k-1) + \qquad (26)$$
$$\mathcal{B}(k)\hat{U}(k-1) + \mathcal{C}(k),$$

where

$$\mathcal{A}(k) \triangleq \mathcal{H}^{\mathrm{T}}\mathcal{H} + \eta(k)I_{l_U},$$
$$\mathcal{B}(k) \triangleq 2\mathcal{H}^{\mathrm{T}}[z(k) - \mathcal{H}U(k-1)],$$
$$\mathcal{C}(k) \triangleq e^2(k) - 2e(k)\mathcal{H}U(k-1)$$
$$+ U^{\mathrm{T}}(k-1)\mathcal{H}^{\mathrm{T}}\mathcal{H}U(k-1).$$

If either $\mathcal{H}$ has full column rank or $\eta(k) > 0$, then $\mathcal{A}(k)$ is positive definite. In this case, $\bar{J}(\hat{U}(k-1),k)$ has the unique global minimizer

$$\hat{U}(k-1) = -\frac{1}{2}\mathcal{A}^{-1}(k)\mathcal{B}(k). \qquad (27)$$

Next, let d be a positive integer such that $U(k-1)$ contains $u(k-d)$ and define the cumulative cost function

$$J(\theta,k) \triangleq \sum_{i=d+1}^{k} \lambda^{k-i}\|\phi^{\mathrm{T}}(i-d-1)\theta^{\mathrm{T}}(k) - \hat{u}^{\mathrm{T}}(i-d)\|^2$$
$$+ \lambda^k(\theta(k) - \theta(0))P^{-1}(0)(\theta(k) - \theta(0))^{\mathrm{T}}, \qquad (28)$$
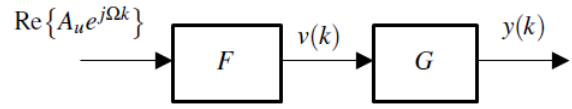
Fig. 6. A model of the Hammerstein system presented with the describing function F, which approximates the input nonlinearity $\mathcal{N}$ under the harmonic input $\mathrm{Re}\{A_u e^{j\Omega k}\}$.

where $\|\cdot\|$ is the Euclidean norm, and $\lambda \in (0,1]$ is the forgetting factor. Minimizing (28) yields

$$\theta^{\mathrm{T}}(k) = \theta^{\mathrm{T}}(k-1) + P(k-1)\phi(k-d-1)$$
$$\times [\phi^{\mathrm{T}}(k-d)P(k-1)\phi(k-d-1) + \lambda(k)]^{-1}$$
$$\times [\phi^{\mathrm{T}}(k-d-1)\theta^{\mathrm{T}}(k-1) - \hat{u}^{\mathrm{T}}(k-d)]. \qquad (29)$$

The error covariance is updated by

$$P(k) = \lambda^{-1}P(k-1) - \lambda^{-1}P(k-1)\phi(k-d-1)$$
$$\times [\phi^{\mathrm{T}}(k-d-1)P(k-1)\phi(k-d) + \lambda]^{-1}$$
$$\times \phi^{\mathrm{T}}(k-d-1)P(k-1). \qquad (30)$$

We initialize the error covariance matrix as $P(0) = \alpha I_{2n_c}$, where $\alpha > 0$.

3.4. Discussion

An input nonlinearity introduces distortion in the loop that gives rise to harmonics of the command frequencies. The goal is thus to determine whether RCAC converges to an approximate IMP control law that compensates for this distortion. We investigate this question in two different ways. First, we examine the required magnitude of the controller to determine whether it provides high gain at the command frequency and harmonics introduced by the input nonlinearity. However, this does not shed light on the phase compensation provided by the controller. In addition, since the input nonlinearity is present in the loop, we no longer expect G_{ur} and G to be mutual inverses at the command frequency. To circumvent this problem, we turn to describing functions [18] to approximate the phase and magnitude of the input nonlinearity at the command frequency, see Fig. 6. In particular, we ask the following question: Does RCAC converge to a controller with the property that G_{ur} and FG are approximate mutual inverses at the command frequency? Here F denotes the describing function of the input nonlinearity. In the case of memoryless input nonlinearities, the describing function is independent of frequency and is real, that is, the describing function models zero phase shift. The objective is to determine whether RCAC can achieve IMP control in the presence of an unknown memoryless input nonlinearity. To investigate this, we examine the magnitude and

phase of

$$G_{ur}(e^{j\Omega}) \triangleq \frac{G_{c,2000}(e^{j\Omega})}{1 + F(|A_u|)G(e^{j\Omega})G_{c,2000}(e^{j\Omega})}. \quad (31)$$

The magnitude $|G_{ur}(e^{j\Omega})|$ reveals whether the controller $G_{c,2000}(e^{j\Omega})$ provides high magnitude at the command frequencies and their harmonics introduced by the Hammerstein system in Fig. 6. The phase $\angle G_{ur}(e^{j\Omega})$ shows whether $G_{c,2000}(e^{j\Omega})$ compensates the phase shift provided by the Hammerstein system in Fig. 6 at the command frequency. To regulate the command-following error e to 0 at the frequency Ω, it follows from

$$r(k) = G(e^{j\Omega})F(|A_u|)G_{ur}(e^{j\Omega})r(k), \quad (32)$$

that

$$G(e^{j\Omega})F(|A_u|)G_{ur}(e^{j\Omega}) = 1. \quad (33)$$

The gain and phase of G_{ur} therefore must satisfy

$$|G_{ur}(e^{j\Omega})| = \frac{1}{F|A_u||G(e^{j\Omega})|}, \quad (34)$$

$$\angle G_{ur}(e^{j\Omega}) = -\angle G(e^{j\Omega}). \quad (35)$$

4. NUMERICAL EXAMPLES

4.1. Linear system with RCAC

Example 2: Consider Example 1 using RCAC with $n_c = 6$, $\alpha = 3$, $d = 1$, and $\lambda = 1$. Fig. 7(c) indicates the magnitudes $|G_{ur}(e^{j\frac{\pi}{5}})| = -5.157$ dB and $|G(e^{j\frac{\pi}{5}})| = 5.158$ dB, and phase angles $\angle G_{ur}(e^{j\frac{\pi}{5}}) = 97.27$ deg and $\angle G(e^{j\frac{\pi}{5}}) = -97.28$ deg. It can be concluded that G_{ur} with $G_{c,2000}$ inverts the plant G at the command frequency Ω.

4.2. Hammerstein Plants with a deadzone nonlinearity

In this section we consider the deadzone input nonlinearity, shown in Fig. 8, for the closed-loop system shown in Fig. 5. Then,

$$\mathcal{N}(u) = \max\{u - \sigma, \min\{u + \sigma, 0\}\}, \quad (36)$$

where σ is a positive constant.

Example 3: We consider the command $r(k) = \sin(\frac{\pi}{5}k)$, the deadzone nonlinearity (36) with $\sigma = 0.25$, the asymptotically stable linear plant $G(z) = \frac{z-0.5}{(z-0.8)(z-0.6)}$, and the Lyapunov-stable plant $G(z) = \frac{1}{z-1}$. We use RCAC with $n_c = 13$, $\alpha = 6$, $d = 1$, and $\lambda = 1$. Fig. 9 shows the simulation results. The choice of controller order is necessitated by the harmonics due to the input nonlinearity.

Example 3 shows that RCAC stabilizes the closed-loop system and decreases the command-following error e for the harmonic command r. It remains to be shown that G_{ur} obtained from RCAC inverts the Hammerstein system $\mathcal{H}$
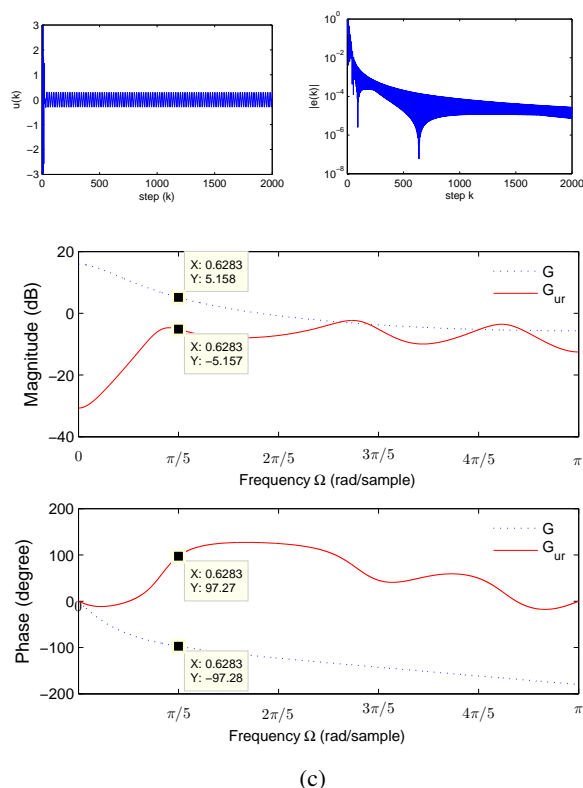
Fig. 7. Example 2: (a) shows the control signal $u(k)$, (b) shows the command-following error $e(k)$, and (c) shows bode plots of G and $G_{ur} = \frac{G_c}{1+GG_c}$. The figure shows that the magnitude and phase of G_{ur} compensate for the magnitude and phase of G at $\Omega = \pi/5$ rad/sample.
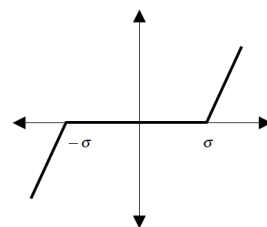
Fig. 8. The deadzone nonlinearity with threshold σ.

considered in Example 3. We use the describing function for the deadzone nonlinearity to investigate this question. With $r(k) = \text{Re}\{A_r e^{j\Omega k}\}$, the output of the Hammerstein system $\mathcal{H}$ with input deadzone nonlinearity can be approximated by the describing function

$$F(|A_u|) = \frac{2\kappa}{\pi}\left(\frac{\pi}{2} - \sin^{-1}\eta_\sigma - \eta_\sigma\sqrt{1 - \eta_\sigma^2}\right), \quad (37)$$

where $\eta_\sigma \triangleq \frac{\sigma}{A_u}$. It follows from (33) that the gain and phase of G_{ur} therefore must satisfy (34) and (35). Fig. 10(a) shows the magnitude $F(|A_u|) = -1.155$, $|G(e^{j\frac{\pi}{5}})| = 5.158$, and $|G_{ur}(e^{j\frac{\pi}{5}})| = -4.008$ dB $\cong -(|G_{ur}| + F(|A_u|))$

(a)   (b)

(c)   (d)
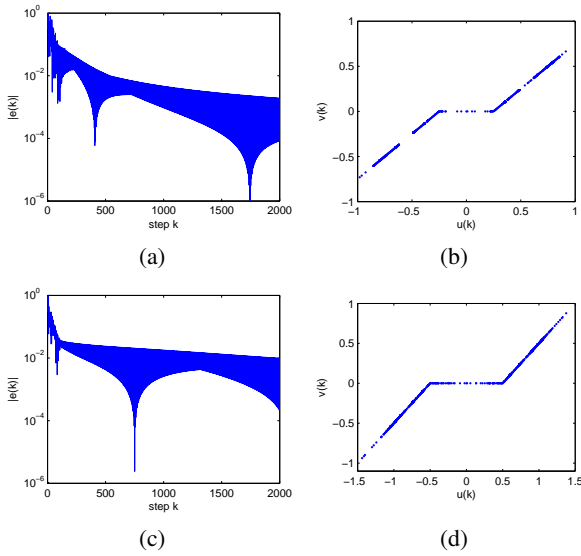
Fig. 9. Example 3: (a) shows the command-following error e for the asymptotically stable linear plant $G(z) = \frac{z-0.5}{(z-0.8)(z-0.6)}$ with the deadzone nonlinearity (36), (b) shows $v(k)$ versus $u(k)$, (c) shows the command-following error e for the Lyapunov-stable plant $G(z) = \frac{1}{z-1}$ with the deadzone nonlinearity (36), and (d) shows $v(k)$ versus $u(k)$. The results show that RCAC stabilizes the closed-loop system and decreases the command-following error e for the harmonic command r.

and phase $\angle G(e^{j\frac{\pi}{5}}) = -97.28$ deg $\angle G_{ur}(e^{j\frac{\pi}{5}}) = 97.34$ deg $= -\angle G(e^{j\frac{\pi}{5}})$. Hence Fig. 10(a) shows that G_{ur} with $G_{c,2000}$ inverts the phase and magnitude of the Hammerstein system in Example 3. Fig. 10(b) shows that G_{ur} with $G_{c,2000}$ inverts the phase and the magnitude of the Hammerstein system $\mathcal{H}$ for the Lyapunov-stable plant $G(z) = \frac{1}{z-1}$.

4.3. Hammerstein plants with a cubic nonlinearity

In this section we consider the cubic nonlinearity

$$\mathcal{N}(u) = u^3. \tag{38}$$

Example 4: We consider the command $r(k) = \sin(\frac{\pi}{5}k)$, the cubic nonlinearity (38), and the stable plant $G(z) = \frac{z-0.5}{(z-0.8)(z-0.6)}$ and the Lyapunov-stable plant $G(z) = \frac{1}{z-1}$, and RCAC with $n_c = 14$, $\alpha = 1$, $d = 1$, and $\lambda = 1$. Fig. 11 shows the simulation results.

We investigate whether RCAC inverts the Hammerstein system $\mathcal{H}$ considered in Example 4. With $r(k) = \text{Re}\{A_r e^{j\Omega k}\}$, the output of the Hammerstein system $\mathcal{H}$ with input deadzone nonlinearity can be approximated by [18]

$$F(|A_u|) = \frac{3}{4}|A_u|^2. \tag{39}$$

(a)

(b)
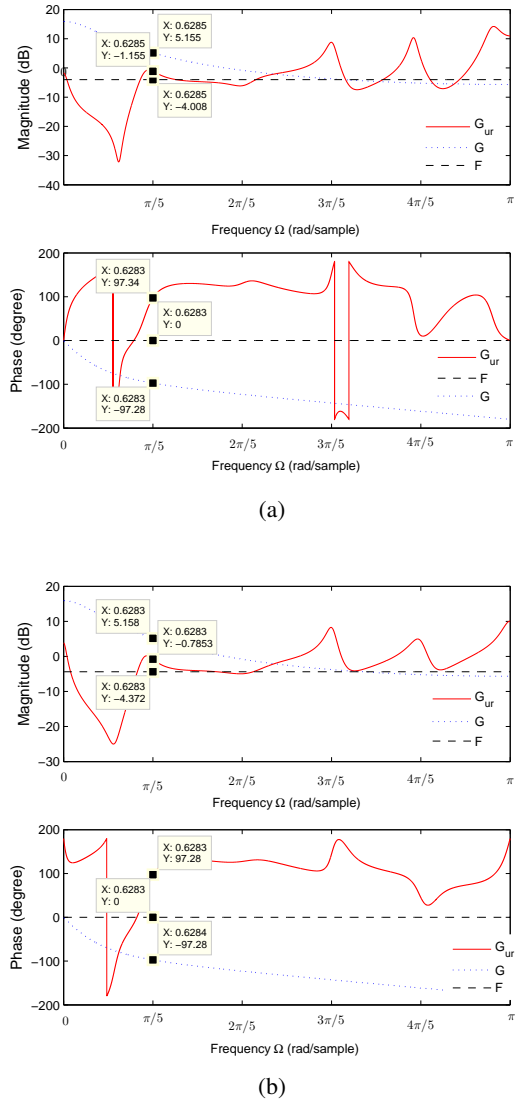
Fig. 10. Bode plots for Example 3: (a) and (b) show the frequency of G_{ur}, G, and the describing function F of the deadzone nonlinearity with (a) the asymptotically stable linear plant $G(z) = \frac{z-0.5}{(z-0.8)(z-0.6)}$, and (b) the Lyapunov-stable plant $G(z) = \frac{1}{z-1}$. The figure shows that the magnitude and phase of G_{ur} compensate for the magnitude and phase of FG at $\Omega = \pi/5$ rad/sample.

It follows from (33) that the gain and phase of G_{ur} therefore must satisfy (34) and (35). Fig. 12(a) shows the magnitude $|G(e^{j\frac{\pi}{5}})| = 4.18$ dB, $F(|A_u|) = -5.53$ dB, and $|G_{ur}(e^{j\frac{\pi}{5}})| = 1.634$ dB $\cong -(F(|A_u|) + |G(e^{j\frac{\pi}{5}})|)$, and phase $\angle G_{ur}(e^{j\frac{\pi}{5}}) = 108$ deg and $\angle G(e^{j\frac{\pi}{5}}) = -108$ deg $= -\angle G_{ur}(e^{j\frac{\pi}{5}})$. Hence, Fig. 12(a) shows that G_{ur} inverts the phase and magnitude of the Hammerstein system $\mathcal{H}$ presented in Example 4. Fig. 12(b) shows that G_{ur} with $G_{c,2000}$ inverts the phase and magnitude of the Hammer-

(a)   (b)

(c)   (d)
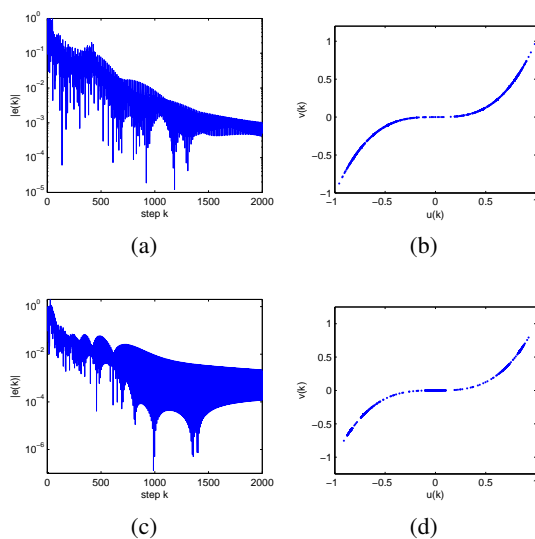
Fig. 11. Example 4: (a) shows the command following error e for the asymptotically stable linear plant $G(z) = \frac{z-0.5}{(z-0.8)(z-0.6)}$ with the cubic nonlinearity (38), (b) shows $v(k)$ versus $u(k)$, (c) shows the command following error e for the Lyapunov-stable plant $G(z) = \frac{1}{z-1}$ with the cubic nonlinearity (38), and (d) shows $v(k)$ versus $u(k)$. The results show that RCAC stabilizes the closed-loop system and decreases the command-following error e for the harmonic command r.

stein system $\mathcal{H}$ for the asymptotically stable linear plant $G(z) = \frac{z-0.5}{(z-0.8)(z-0.6)}$.

4.4. Hammerstein plants with a saturation nonlinearity

In this section we consider the closed-loop system shown in Fig. 5 with the saturation nonlinearity

$$\mathcal{N}(u) = \begin{cases} \kappa, & \text{if } u \geq \kappa, \\ u, & \text{if } -\kappa \leq u \leq \kappa, \\ -\kappa & \text{if } u \leq \kappa, \end{cases} \quad (40)$$

where κ is a positive constant.

Example 5: We consider the command $r(k) = 1.75\sin(\frac{\pi}{10}k)$, the saturation nonlinearity (40), the unstable plant $G(z) = \frac{1}{z-1.1}$, and the asymptotic stable plant $G(z) = \frac{1}{z-0.7}$. We consider RCAC with $n_c = 6$, $\alpha = 0.2$, $d = 1$, and $\lambda = 1$. Fig. 14 shows the simulation results.

We investigate whether RCAC inverts the Hammerstein system $\mathcal{H}$ considered in Example 5. With $r(k) = \text{Re}\{A_r e^{j\Omega k}\}$, the output of the Hammerstein system $\mathcal{H}$ with input saturation nonlinearity can be approximated by

(a)

(b)
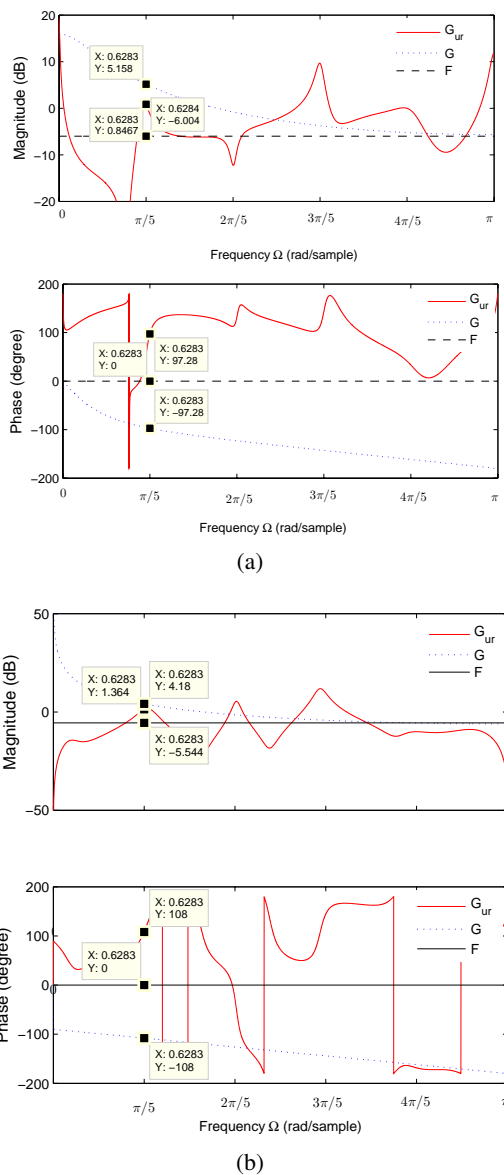
Fig. 12. Bode plots for Example 4: (a) and (b) show the frequency of G_{ur}, G, and the describing function F of the cubic nonlinearity (38) with (a) the asymptotically stable linear plant $G(z) = \frac{z-0.5}{(z-0.8)(z-0.6)}$, and (b) the Lyapunov-stable plant $G(z) = \frac{1}{z-1}$. The figure shows that the magnitude and phase of G_{ur} compensate the magnitude and phase of FG at $\Omega = \pi/5$ rad/sample.

the describing function [18]

$$F(|A_u|) = \frac{2}{\pi}\left(\sin^{-1}(\frac{a}{A}) + \frac{a}{A}\sqrt{1 - \frac{a^2}{A^2}}\right). \quad (41)$$

It follows from (33) that the gain and phase of G_{ur} therefore must satisfy (34) and (35). Fig. 15(a) shows the magnitude $F(|A_u|) = 11.48$ dB, $|G(e^{j\frac{\pi}{10}})| = 14.47$ dB, and
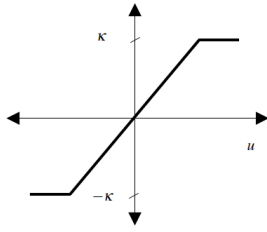
Fig. 13. The saturation nonlinearity with threshold κ.

(a)   (b)

(c)   (d)
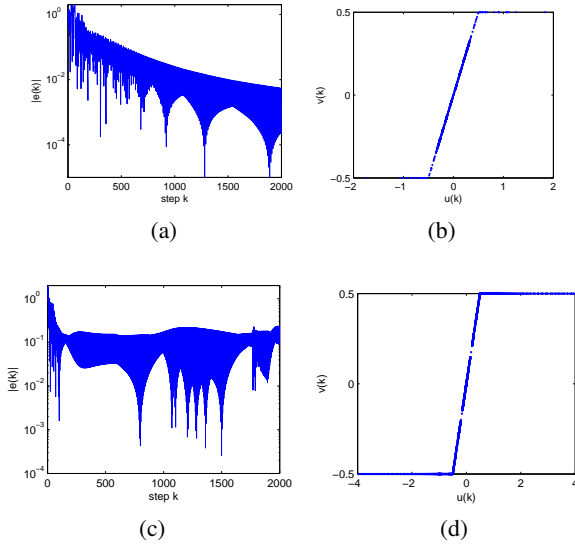
Fig. 14. Example 5: (a) shows the command-following error e for the stable linear plant $G(z) = \frac{z-0.7}{(z-0.95)(z-0.8)}$ with the saturation nonlinearity (40), (b) shows $v(k)$ versus $u(k)$, (c) shows the command following error e for the unstable plant $G(z) = \frac{1}{z-1.1}$ with the saturation nonlinearity (40), and (d) shows $v(k)$ versus $u(k)$. The results show that RCAC stabilizes the closed-loop system and decreases the command-following error e for the harmonic command r.

$|G_{ur}(e^{j\frac{\pi}{10}})| = -25.94$ dB $\cong -(|G(e^{j\frac{\pi}{10}})| + F(|A_u|))$, and phase $\angle G_{ur}(e^{j\frac{\pi}{5}}) = 103.1$ deg and $\angle G(e^{j\frac{\pi}{5}}) = -102.6$ deg $\cong -\angle G_{ur}(e^{j\frac{\pi}{5}})$. Hence, Fig. 15(a) shows that G_{ur} with $G_{c,2000}$ inverts the magnitude and phase of the Hammerstein system $\mathcal{H}$ presented in Example 5. Fig. 15(b) shows that G_{ur} with $G_{c,2000}$ inverts the phase and magnitude of the Hammerstein system $\mathcal{H}$ for the unstable plant $G(z) = \frac{1}{z-1.1}$.

5. RCAC FOR HAMMERSTEIN SYSTEM WITH BACKLASH NONLINEARITY

In this section we consider the backlash input nonlinearity for the closed-loop system shown in Fig. 5. Let

$$\mathcal{N}(k) = \mathcal{B}[u](k) \tag{42}$$

(a)

(b)
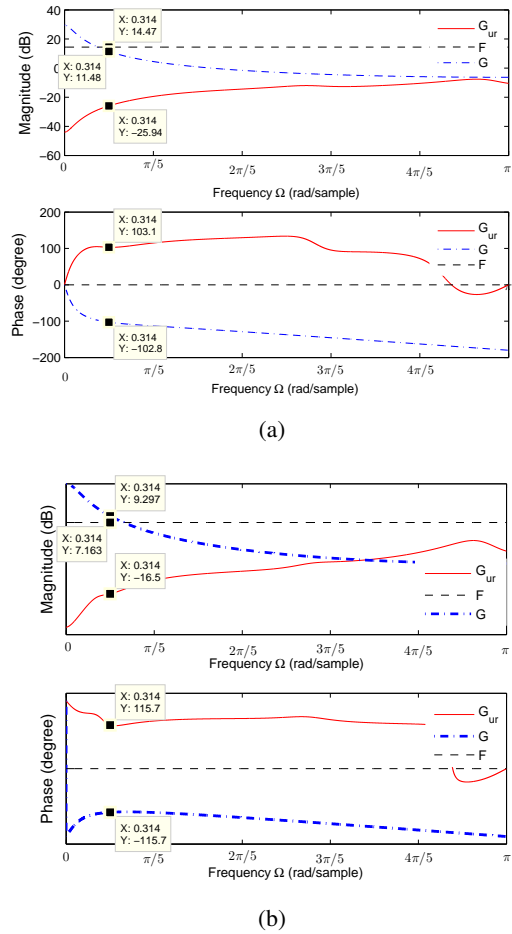
Fig. 15. Bode plots for Example 5: (a) and (b) show the frequency of G_{ur}, G, and the describing function F of the saturation nonlinearity with (a) the stable linear plant $G(z) = \frac{z-0.7}{(z-0.95)(z-0.8)}$, and (b) the unstable plant $G(z) = \frac{1}{z-1.1}$. The figure shows that the magnitude and phase of G_{ur} compensate the magnitude and phase of FG at $\Omega = \pi/10$ rad/sample.

and $\mathcal{B}[u](k) = b_\rho(k)$, where

$$b_\rho(k) = \max\{\kappa(u(k) - \rho), \min\{\kappa(u(k) + \rho), b_\rho(k-1)\}\}, \tag{43}$$

where $b_\rho(1) = \max\{\kappa(u(1) - \rho), \min\{\kappa(u(1) + \rho), 0\}\}$, ρ is a positive threshold, and κ is a positive constant determents the slope of the increasing $(u(k) - \rho)$ and decreasing $(u(k) + \rho)$ curves.

In the following example we show that the RCAC minimizes the command-following error e when the input backlash nonlinearity $\mathcal{B}$ is considered.

Example 6: We consider the command $r(k) = \sin(\frac{\pi}{5}k)$, the backlash operator $\mathcal{B}$ with $\rho = 0.4$, the asymptotically stable linear plant $G(z) = \frac{z-0.5}{(z-0.8)(z-0.6)}$, and the Lyapunov stable plant $G(z) = \frac{1}{z-1}$. We use RCAC with $n_c = 12$, $\alpha =$

(a)　　　　　　　　　(b)

(c)　　　　　　　　　(d)
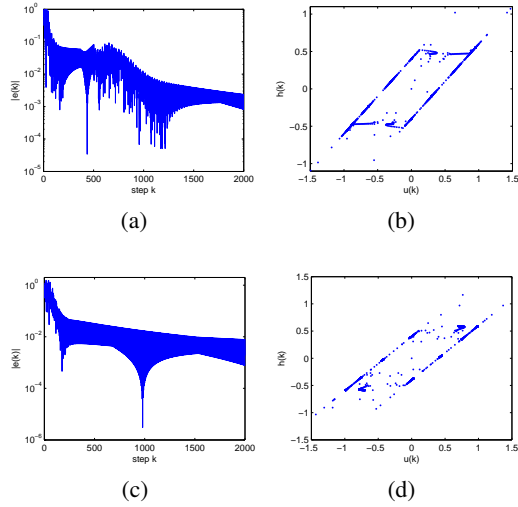
Fig. 16. Example 6: (a) shows the command following error e when the asymptotically stable linear plant $G(z) = \frac{z-0.5}{(z-0.8)(z-0.6)}$ and the output of the backlash operator $\mathcal{B}$ shown in (b) considered in the closed-loop system with RCAC, (c) shows the command following error e when the Lyapunov stable plant $G(z) = \frac{1}{z-1}$ and the output of the backlash operator $\mathcal{B}$ shown in (d) considered in the closed-loop system with RCAC.

3, $d = 1$, and $\lambda = 1$. Fig. 9 shows the simulation results.

The closed-loop system constructed with the RCAC decreases the command-following error e and stabilizes the closed-loop system with the harmonic command r is considered. We use the describing function for the backlash to explain that compensation in the closed-loop system.

$$y(k) \cong \text{Re}\left\{ A_r |G_{ur}(e^{j\Omega})||G(e^{j\Omega})||F(|A_u|)| \right.$$
$$\left. e^{j(\Omega k + \angle F(|A_u|) + \angle G(e^{j\Omega}) + \angle G_{ur}(e^{j\Omega}))} \right\}, \quad (44)$$

where $|F(|A_u|)|$ and $\angle F(|A_u|)$ are the amplitude and the phase of the describing function of the backlash operator, where [18]

$$|F(|A_u|)| = \frac{1}{|A_u|}\sqrt{a_1^2 + b_1^2}, \quad (45)$$

$$\angle F(|A_u|) = \tan^{-1}\frac{a_1}{b_1}, \quad (46)$$

where

$$a_1 = \frac{4\kappa\rho}{\pi}\left(\frac{\rho}{|A_u|} - 1\right), \quad (47)$$

$$b_1 = \frac{|A_u|\kappa}{\pi}\left(\frac{\pi}{2} - \sin^{-1}\eta_\rho - \eta_\rho\sqrt{1 - \eta_\rho^2}\right), \quad (48)$$

where $\eta_\rho = \frac{2\rho}{|A_u|} - 1$. Based on the bode plots presented in Fig. 17, we can conclude that G_{ur} inverts the phase and magnitude of the Hammerstein system $\mathcal{H}$ presented

(a)

(b)
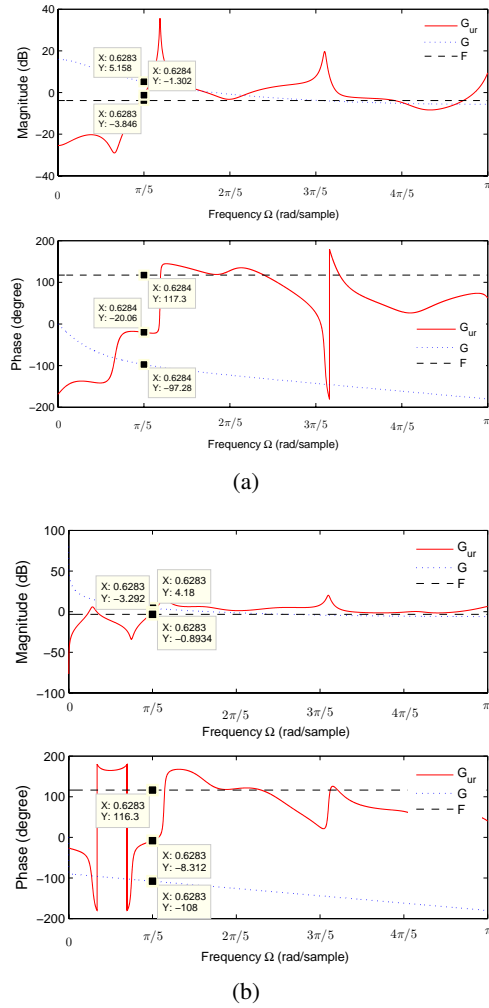
Fig. 17. Example 6: (a) and (b) show the bode plots of G_{ur}, G, and the describing function F of the backlash nonlinearity with (a) the asymptotically stable linear plant $G(z) = \frac{z-0.5}{(z-0.8)(z-0.6)}$, and (b) the Lyapunov stable plant $G(z) = \frac{1}{z-1}$.

in Example 6. Considering the asymptotically stable linear plant $G(z) = \frac{z-0.5}{(z-0.8)(z-0.6)}$, we obtain, (i) the magnitude $|G_{ur}(e^{j\frac{\pi}{5}})| = -1.308$ dB, $|F(|A_u|)| = -3.846$ dB, and $|G(e^{j\frac{\pi}{5}})| = 5.158$ dB, and (ii) the phase $\angle G_{ur}(e^{j\frac{\pi}{5}}) = -20.06$ deg, $\angle G(e^{j\frac{\pi}{5}}) = -97.28$ deg, and $\angle F(|A_u|) = 117.3$ deg. Fig. 17(b) shows that G_{ur} inverts the phase and magnitude of the Hammerstein system $\mathcal{H}$ with the backlash input nonlinearity with $\rho = 0.4$ when the Lyapunov stable plant $G(z) = \frac{1}{z-1}$ is considered.

6. CONCLUSIONS

The numerical investigation carried out in the paper shows that the adaptive control law can achieve IMP control in the presence of plant input nonlinearities. For memoryless nonlinearities, RCAC was shown to invert

the Hammerstein system at the command frequency of the harmonic command input. It is important to note that the investigation in this paper is numerical, and is intended to motivate theoretical studies of adaptive control of Hammerstein systems with harmonic commands and disturbances. We stress that the diagnostics that we use are not confined to RCAC, but can be used to investigate the asymptotic properties of any control law that is applicable to either command following (possibly MRAC) or disturbance rejection. In addition, this paper shows that the classical technique of describing functions can shed light on the properties of adaptive control laws.

REFERENCES

[1] B. Francis and W. Wonham, "The internal model principle of control theory," *J. Appl. Mtah. Optim.*, vol. 2, no. 5, 170-194, 1975.

[2] E. J. Davison, "The robust control of a servomechanism problem for linear time-invariant multivariable systems," *IEEE Trans. Automat. Contr.*, vol. AC-21, pp. 25-34, 1976.

[3] C. Li and Y. Wang, "Input disturbance suppression for port-controlled hamiltonian system via the internal model method," *Int. J. Contr., Autom. and Sys.*, vol. 11, no. 2, pp. 268-276, 2013.

[4] K. J. Astrom and T. Hagglund, *Advanced PID Control*, ISA, Research Triangle Park, NC, 2006.

[5] J. Yan and D. S. Bernstein, "Minimal modeling retrospective cost adaptive control of uncertain hammerstein systems using auxiliary nonlinearities," *Int. J. Contr.*, Vol. 87, pp. 483-505, 2014.

[6] M. Al Janaideh and D. S. Bernstein, "A numerical investigation of phase and magnitude compensation in adaptive control of uncertain hammerstein systems with hysteretic nonlinearities," *Proc. Amer. Contr. Conf.*, Portland, OR, pp. 2014.

[7] M. Al Janaideh and D. S. Bernstein, "Adaptive control of hammerstein systems with unknown prandtl-Ishlinskii hysteresis," *Proceedings of the Institution of Mechanical Engineers, Part I: Journal of Systems and Control Engineering*, vol. 229, no. 2, pp. 149-157, 2015.

[8] A. Goel, A. Xie, K. Duraisamy, and D. S. Bernstein, "Retrospective cost adaptive thrust control of a 1D scramjet with mach number disturbance," *Proc. Amer. Contr. Conf.*, pp. 5551-5556, Chicago, IL, July 2015.

[9] F. Sobolic and D. S. Bernstein, "An inner-loop/iuter-loop architecture for an adaptive missile autopilot," *Proc. Amer. Contr. Conf.*, pp. 850-855, Chicago, IL, July 2015.

[10] M. C. Kung and B. F. Womack, "Discrete-time adaptive control of linear dynamic systems with a two-segment piecewise-linear asymmetric nonlinearity," *IEEE Trans. Autom. Contr.*, vol. 29, no. 2, pp. 170-172, 1984.

[11] M. C. Kung and B. F. Womack, "Discrete-time adaptive control of linear systems with preload nonlinearity," *Automatica*, vol. 20, no. 4, pp. 477-479, 1984.

[12] G. Tao and P. V. Kokotović, *Adaptive Control of Systems with Actuator and Sensor Nonlinearities*, Wiley, 1996.

[13] J. Yan, A. M. D'Amato, D. Sumer, J. B. Hoagg, and D. S. Bernstein, "Adaptive control of uncertain hammerstein systems using auxiliary nonlinearities," *Proc. Conf. Dec. Contr.*, Maui, HI, pp. 4811-4816, 2012.

[14] M. Al Janaideh, J. Yan, A. M. D'Amato, and D. S. Bernstein, "Retrospective-cost adaptive control of uncertain hammerstein-wiener systems with memoryless and hysteretic nonlinearities," *AIAA Guid. Nav. Contr. Conf.*, Minneapolis, MN, AIAA-2012-4449-671, August 2012.

[15] R. Venugopal and D. S. Bernstein, "Adaptive disturbance rejection using ARMARKOV system representations," *IEEE Trans. Contr. Sys. Tech.*, vol. 8, pp. 257-269, 2000.

[16] J. B. Hoagg, M. A. Santillo, and D. S. Bernstein, "Discrete-time adaptive command following and disturbance rejection for minimum-phase systems with unknown exogenous dynamics," *IEEE Trans. Autom. Contr.*, vol. 53, pp. 912-928, 2008.

[17] A. M. D'Amato, E. D. Sumer, and D. S. Bernstein, "Frequency-domain stability analysis of retrospective-cost adaptive control for systems with unknown nonminimum-phase zeros," *Proc. Conf. Dec. Contr.*, Orlando, FL, pp. 1098-1103, 2011.

[18] J. Slotine and W. Li, *Applied Nonlinear Control*, Prentice-Hall, NJ, 1991.

Mohammad Al Janaideh received the MASc. and Ph.D. degrees in mechanical engineering and mechatronics from Concordia University, Montreal, Quebec, Canada, in 2005 and 2009, respectively. He held research and teaching positions in various countries, including Canada, Jordan, Italy, the USA, and Czech Republic. He joined the Department of Aerospace Engineering, University of Michigan, Ann Arbor, MI, USA, as a Visiting Scholar in 2013. He is with the Department of Mechanical Engineering at University of Toronto. His research interests include control of mechatronics systems, control of systems with hysteresis, adaptive control for nonlinear systems, modeling and control of pneumatic artificial muscles, and design of MEMS sensors.

Dennis S. Bernstein received the Sc.B. degree in applied mathematics from Brown University in 1977 and the Ph.D. degree in control engineering from the University of Michigan in Ann Arbor, Michigan, in 1982, where he is currently professor in the Aerospace Engineering Department. His interests are in estimation, identification, and control for aerospace applications. He is the author of Matrix Mathematics: Theory, Facts, and Formulas, published by Princeton University Press.